2-1-2022

β-Aminopropionitrile-Induced Aortic Aneurysm and Dissection in Mice

Hisashi Sawada
University of Kentucky, hisashi.sawada@uky.edu

Zachary A. Beckner
University of Kentucky, Zachary.Beckner@uky.edu

Sohei Ito
University of Kentucky, sohei.ito@uky.edu

Alan Daugherty
University of Kentucky, alan.daugherty@uky.edu

Hong S. Lu
University of Kentucky, hong.lu@uky.edu

β-Aminopropionitrile-Induced Aortic Aneurysm and Dissection in Mice

Digital Object Identifier (DOI)
https://doi.org/10.1016/j.jvssci.2021.12.002

Notes/Citation Information
Published in *JVS: Vascular Science*, v. 3.

β-Aminopropionitrile-induced aortic aneurysm and dissection in mice

Hisashi Sawada, MD, PhD,[a,b,c] Zachary A. Beckner, BS Candidate,[a,b] Sohei Ito, MD, PhD,[a,b] Alan Daugherty, PhD, DSc,[a,b,c] *and* Hong S. Lu, MD, PhD,[a,b,c] *Lexington, Ky*

ABSTRACT

The mechanistic basis for the formation of aortic aneurysms and dissection needs to be elucidated to facilitate the development of effective medications. β-Aminopropionitrile administration in mice has been used frequently to study the pathologic features and mechanisms of aortic aneurysm and dissection. This mouse model mimics several facets of the pathology of human aortic aneurysms and dissection, although many variables exist in the experimental design and protocols that must be resolved to determine its application to the human disease. In the present brief review, we have introduced the development of this mouse model and provided insights into understanding its pathologic features. (JVS—Vascular Science 2022;3:64-72.)

Keywords: β-Aminopropionitrile; Aortic aneurysms; Aortic dissection; Mouse

Aortic aneurysm and dissection (AAD) are devastating diseases. Aortic aneurysms are defined as pathologic luminal dilatations with a high risk of uncontrolled bleeding due to aortic rupture and death.[1-3] Aortic aneurysms are most common in the infrarenal abdominal aortic region,[4] with the proximal thoracic aortic region as the second most common location.[5,6] Aortic dissection leads to bleeding into the medial layers in the thoracic aorta and can extend into the abdominal aorta, causing organ malperfusion with critical consequences.[1-3] Surgical procedures have been the primary therapy because no medications have been proved effective. Therefore, research using animal models that mimic facets of the human disease will hopefully provide mechanistic insights that will lead to a path for the development of effective medical therapies.

Although many animal models of AAD have been developed, an increasingly common model is based on the administration of β-aminopropionitrile (BAPN) in mice. One premise for developing this model was the observation that turkeys died of aortic rupture after eating sweet peas, with the subsequent identification of BAPN as the active constituent.[7,8] The mechanistic basis for BAPN-induced aortopathy was proposed to be the inhibition of lysyl oxidase (LOX) activity, which catalyzed crosslinking of lysine residue in elastin and collagens to form desmosine. These extracellular matrix proteins are crucial components for maintaining aortic integrity.[9-11] Several studies have demonstrated that chronic BAPN administration results in AAD formation in mice, providing a model to investigate the pathophysiology and mechanisms of AAD.[12-14] BAPN administration has been used frequently with angiotensin II (AngII) infusion to promote AAD formation in mice. However, BAPN administration alone can also induce heterogeneous aortic pathologies that mimic facets of the human disease. In the present review, we have highlighted studies that used BAPN as the only chemical intervention to induce AAD in mice, summarized the BAPN-induced AAD pathologies and their detection using imaging modalities, and provided suggestions for optimal experimental designs.

DEVELOPMENT OF BAPN-INDUCED AAD IN MICE

Effects of BAPN on LOX and LOX-like proteins. LOX and LOX-like protein (LOXL) family members, LOXL1 to LOXL4, are essential enzymes for the crosslinking of elastin and collagens.[15] LOX-deficient mice exhibit disrupted elastin and collagen crosslinking.[16] However, no studies have investigated AAD in mice deficient in any of the LOXL proteins. A missense mutation in LOX has been identified in patients with AAD that was replicated in a mouse model with this LOX mutation.[17] These findings support the notion that disruption of LOX contributes to the formation of AAD.

From the Saha Cardiovascular Research Center,[a] Saha Aortic Center,[b] and Department of Physiology,[c] University of Kentucky.

The authors' aortic aneurysm-related research is supported by the National Heart, Lung, and Blood Institute, National Institutes of Health (grants R01HL133723 and R35HL155649), and the American Heart Association Vascular Disease Strategically Focused Research Network (grant 18SFRN33960163). The content in our report is solely the responsibility of the authors and does not necessarily represent the official views of the National Institutes of Health.

Author conflict of interest: none.

Correspondence: Hong S. Lu, MD, PhD,; Alan Daugherty, Saha Cardiovascular Research Center, University of Kentucky, Biomedical/Biological Sciences Research Building, Rm 249, 741 S Limestone, Lexington, KY 40536-0509 (e-mail: hong.lu@uky.edu).

The editors and reviewers of this article have no relevant financial relationships to disclose per the JVS-Vascular Science policy that requires reviewers to decline review of any manuscript for which they may have a conflict of interest.

2666-3503

https://doi.org/10.1016/j.jvssci.2021.12.002

BAPN was reported initially as an irreversible pharmacologic inhibitor of LOX and LOXL proteins.[18-20] BAPN decreased LOX activity, as demonstrated using purified LOX from bovine aortas or chick cartilages.[18,19] An in vitro study using *Escherichia coli* showed that LOXL1 and LOXL2 were also inhibited by BAPN.[20] However, a recent report demonstrated that BAPN inhibited LOXL2 effectively in vitro but not LOX.[21] No studies have reported the contribution of LOXL2 to AAD using in vivo models. Further study is needed to provide a consensus of which enzymes in the LOX/LOXL family are inhibited by BAPN. In addition, more insight is required regarding the roles of LOXL enzymes in AAD pathophysiology.

BAPN administration. Many of the initial studies had induced aortopathies by a combination of BAPN administration with another mode of provoking AAD. This was initially demonstrated by coadministration of BAPN and AngII, which induced AAD in adult male C57BL/6J mice.[22,23] Adult mice had not shown overt aortic pathologies when BAPN was administered alone.[22] Subsequent studies have demonstrated that BAPN administration combined with other manipulations will induce AAD in adult mice, including application of elastase to the adventitia of the infrarenal aorta or administration of DOCA (deoxycorticosterone acetate)-salt.[22,24,25] Among these manipulations, AngII infusion has been used most often in conjunction with BAPN to enhance AAD formation. In young (3-week-old) mice, AAD formation was observed with a 100% incidence when BAPN was administered for 4 weeks with an AngII (1 μg/kg/min) infusion for 24 hours before termination.[12] In 3- to 4-week-old mice after 3 to 4 weeks of BAPN administration, AngII infusion for 12, 24, and 48 hours led to death due to rupture at an incidence of 14% (7 of 50), 39% (18 of 46), and 67% (29 of 43), respectively.[26] Therefore, studies have demonstrated consistently that transient AngII infusion augments BAPN-induced AAD.

Accumulating evidence has shown that BAPN administration alone will induce AAD formation in young mice. In one study, 3-week-old male C57BL/6 mice had >80% AAD formation during BAPN administration without other manipulations.[12] BAPN administration started at 3 to 4 weeks of age suppressed elastogenesis but did not induce elastolysis.[27] BAPN irreversibly inhibits crosslinking of elastin and collagen. However, crosslinking of elastin and collagen is presumed to be minimal after the postnatal phase. Thus, inhibition of LOX/LOXL activity might not disrupt already formed elastic fibers. Patients with connective tissue disease, such as Marfan syndrome, Ehlers-Danlos syndrome, or Turner syndrome, often develop the complication of aortic dissection. The incidence of aortic complications peaks at 30 to 40 years of age in patients with these syndromes.[28-30] Because BAPN administration in young mice (age, 3-4 weeks) leads to AAD formation through the inhibition of elastin and collagen crosslinking during extracellular matrix maturation, this mouse model might mimic certain molecular mechanisms of aortic diseases complicated by the connective tissue diseases mentioned above.

Route and dose of BAPN administration. BAPN has been administered in several modes in mouse studies. Mini-osmotic pumps can be used to deliver BAPN to adult mice (age, 7-15 weeks).[22,31-36] However, it has been more common to administer BAPN in the drinking water for young mice (age, 3-4 weeks). A few studies have used BAPN administration via a gastric tube,[26] diet,[12,37] or intraperitoneal injection.[38]

Mini-osmotic pumps provide a constant and continuous delivery of compounds. This approach has been used extensively for delivery of AngII to induce aortic aneurysms in mice.[39,40] Given a previous study demonstrating that the half-life (beta phase) of BAPN was 79 ± 5 minutes in rabbits,[41] subcutaneous infusion using osmotic pumps can be considered an optimal mode for BAPN administration. However, two considerations are important for the use of this mode: the solubility of the compound and the size of the pump. A commonly used infusion rate of BAPN has been 150 mg/kg/d for osmotic pump delivery. This dose requires a highly concentrated BAPN solution (>500 mg/mL) to enable the use of osmotic pumps (pump rate, ~0.25 μL/h; model 2004; ALZET Osmotic Pumps; Durect Corp, Cupertino, Calif). Since the maximal solubility of BAPN in water is ~50 mg/mL, it is challenging to dissolve BAPN (150 mg/kg/d) completely. In addition, the most commonly used osmotic pump, ALZET model 2004, is not recommended for use with mice weighing <20 g, which is incompatible with its use in young mice. Therefore, it is often not feasible to deliver BAPN via an osmotic pump, especially to young mice with a low body weight. Many recent studies have administered BAPN in the drinking water, with AngII delivered through mini-osmotic pumps.[42,43] This method appears to be an optimal mode for the administration of BAPN to young mice.

Multiple studies in which BAPN was administered in drinking water have reported that the dose was 1 g/kg/d (Table I). However, it is unclear how this dose was calculated. This dosage might be appropriate for a mouse weighing ~25 g that drink ~ 5 mL of water daily.[44] However, body weight and water consumption may vary. In addition, mice aged 3 to 4 weeks will weigh 10 to 15 g, and their water consumption can be <5 mL/d. Consequently, an estimated dose of 1 g/kg/d of BAPN is likely to be inaccurate. Therefore, it would be preferable to provide a more direct description of the BAPN dose, such as 1 to 3 mg/mL[42,45,46] or 0.2% to 0.6% [% wt/vol (2-6 mg/mL)] as reported in selected studies.[24,25,43,47-49]

Although the common routes of BAPN administration have been subcutaneous infusion using an osmotic pump or drinking water, other routes have also been

Table I. Administration of BAPN to study AAD in mice

Mouse strain	Sex	Age, weeks	BAPN administration			References
			Route	Dose	Duration, weeks	
C57BL/10	Male	3	Drinking water	0.5 g/kg/d	4	50
C57BL/6[a]	Male	3	Drinking water	1 g/kg/d	2-4	12,51-57
C57BL/6J	Male	3	Drinking water	1 g/kg/d	1, 2, or 4	58-64
FVB	Male	3	Drinking water	1 g/kg/d	4	12
Mixed (C57BL/6[a] and SJL)	Male	3-4	Drinking water	0.3% wt/vol	8-30	45,46
C57BL/6J	Male	3-4	Drinking water	0.5% wt/vol	12	47,48
C57BL/6[a]	Male	3	Drinking water	0.6% wt/vol	4	49
C57BL/6[a]	Male	3	Diet	0.4%, 1%, or 1.5%	4	12

AAD, Aortic aneurysm and dissection; *BAPN*, β-aminopropionitrile.
[a]Substrain of C57BL/6 unknown.

reported, including administration via the diet,[12,37] gastric tube,[26] or intraperitoneal injection.[38] Adding BAPN to the mouse diet had effects similar to that of administering the compound via the drinking water. In the study by Ren et al,[12] mice were fed BAPN at doses of 0.4, 1, or 1.5 g/100 g in their food. All the mice fed 0.4 g/100 g BAPN developed AAD (five died of aortic rupture). In the mice fed 1 g/100 g BAPN, two of six mice had developed thoracic aortic dissection. However, aortic dissection was not observed in the mice fed the highest dose. All BAPN-administered mice had lost body weight in a dose-dependent manner. Although the basis for this body weight loss was not determined, effects of BAPN on the lipid and glucose metabolisms might have contributed to its mechanism.[65,66] Because mixing BAPN in the food is logistically more difficult than dissolving the compound in the drinking water, the latter is an easier approach. Compared with food consumption ad libitum, gastric tube administration and intraperitoneal injection will provide more accurate and consistent administration of BAPN. However, the insertion of a gastric tube is technically demanding and time-consuming. It can also stress the mice, augmenting the formation of AAD and adding a confounding factor. Only one study administered BAPN by intraperitoneal injection, which had focused on aortic stiffness.[38] Thus, the effect of intraperitoneal injection of BAPN on AAD formation has not yet been studied.

Overall, the administration of BAPN (0.5% wt/vol) in the drinking water will induce a high incidence of AAD in young mice (age, 3-4 weeks). Because of the high incidence of AAD formation, this mouse model has facilitated investigations of whether an experimental intervention will attenuate AAD. Since different doses of BAPN can lead to differing severity of AAD, it is important to optimize the BAPN dose before performing experiments.

Mouse strains and sex. The most frequently studied mouse strain has been C57BL/6, with many studies reporting the use of the C57BL/6J substrain. It is important to distinguish between the C57BL/6 substrains. The C57BL/6J and C57BL/6N substrains have well-defined differences, including the recently demonstrated diversity in the development of aortopathies.[67,68] It is also important to consider different mouse strains when designing an experiment because the strains have different susceptibilities to BAPN-induced AAD. Male FVB mice had a lower incidence of AAD compared with age-matched male C57BL/6 mice (substrain not reported): a 25% incidence of AAD and no aortic rupture in FVB mice vs an 87% incidence of AAD and a 37% incidence of aortic rupture in C57BL/6 mice.[12] The high incidence of AAD in C57BL/6 mice has illustrated that the BAPN-induced AAD mouse model does not need a hypercholesterolemic background. However, no studies have determined whether hypercholesterolemia will augment the development of BAPN-induced AAD.

Sexual dimorphism has also been reported in AAD formation in humans and mice.[69-77] In humans, AAD has been more prevalent in men than in women,[69] and the outcomes have frequently been worse for women.[70,71] Women have been shown to be more likely to experience mortality from aortic dissection, lower long-term survival after surgery, and a greater frequency of cardiac complications such as cardiac tamponade.[70-73] In several mouse models, the incidence and severity of abdominal aortic aneurysms are sexually dimorphic, with greater severity in male mice.[74-77] Consistent with this premise, a few studies have reported a lower incidence of AAD in female mice coadministered BAPN and AngII.[43,78] However, no studies have reported on sexual dimorphism when BAPN was administered alone.

PATHOLOGIC FEATURES OF BAPN-INDUCED AAD

Progression of BAPN-induced AAD

Most studies reported AAD formation within 4 weeks of BAPN administration (Table I). No apparent pathologies were noted within 7 days of BAPN administration. However, impairment of the endothelial layer was detected

as early as 7 days after BAPN administration, which was demonstrated with an Evans blue injection into the angular vein 20 minutes before termination.[58] After 7 days of BAPN administration, 00CD45+ cells were detected, mainly in the tunica adventitia, and had increased after 14 days. Neutrophils (Ly6G+ cells) were also detected in the adventitia after 7 days but were not apparent after 14 days of BAPN administration.[59] In addition to the pronounced accumulation of red blood cells, disruption of the elastic fibers was observed after 2 weeks of BAPN administration. Severe fragmentation of the elastic fibers and medial dissection became apparent after 3 weeks of BAPN administration. After 28 days of BAPN administration, the accumulation of leukocytes at the site of medial rupture and the surrounding adventitia was evident.[51-55,59-62,79] For mice surviving 4 weeks of BAPN administration, thrombi had resolved; however, continuous leukocyte infiltration and disorganized collagen deposition were still prominent. After prolonged administration of BAPN for ≤12 weeks,[47,48] pronounced thinning of the aortic wall in the ascending and descending thoracic aortic regions was observed. The prolonged administration of BAPN can cause kyphosis and osteolathyrism in mice.[80] No studies have reported detailed histologic features after protracted intervals of administration.

Tearing of the aortic wall leads to bleeding. If bleeding is constrained by the media or adventitia, thrombi will form, surrounding the ruptured media or adventitia. Aortic rupture occurs if transmural bleeding ensues or the thrombi fail to constrain the blood within the medial and adventitial layers. In BAPN-administered mice, intra- or transmedial dissection was observed, in addition to luminal dilatation, predominantly in the thoracic aorta.[12] The presence of medial dissection and the location of aortic dilatations are distinct pathologic features of this model compared with the AngII-induced abdominal aortic aneurysm model, which demonstrates luminal dilatation with adventitial dissection in the suprarenal abdominal aorta.[40] BAPN-induced AAD has high death rate from aortic rupture. For mice that died of aortic rupture, death has been noted as early as 10 days after the initiation of BAPN and became more frequent after 14 days of BAPN administration. The rate of death from aortic rupture has been reported to be ~ 50% to 80%.[12,52-61,63,64,79]

Although several studies have shown BAPN-induced aortic pathologies at different time points, the systematic determination of the sequential events during BAPN administration from the initiation to the progression of AAD is lacking. The data from previous studies, which usually provided pathology information after a single time point for 3- to 4-week-old mice administered BAPN, have shown that the aortic rupture rate is high. Also, recently formed or resolving hemorrhage in the medial layers has been noted frequently, accompanied by inflammatory cell accumulation, luminal dilation, and profound elastin breaks and extracellular matrix degradation.

Overall, the BAPN-induced AAD mimics several aspects of the heterogeneity of human AAD (Table II). It might be an optimal model to allow us to understand the molecular mechanisms and explore potential therapeutic strategies for AAD. To perform a detailed characterization of the pathologic features over time throughout the diseased regions, it would be helpful to extend the observation period beyond 4 weeks, in addition to the short intervals.

AAD location

Aortic dissection in humans can be categorized into two types: Stanford types A and B. Stanford type A involves the ascending aorta with pathology in the ascending aorta alone or extending to the descending aorta, and type B includes pathologies initiated from the descending aorta. The use of this classification can help to decide the therapeutic strategy. A type A dissection requires urgent surgical repair. In contrast, treatment of type B dissections has not been consistent.[2,3] Therefore, it is important to elucidate the region-specific mechanisms of AAD.

For BAPN-induced AAD, most studies have either focused on thoracic AAD or did not specify the AAD location. One study reported that, in male C57BL/6 mice in which BAPN administration had started at 3 weeks of age, 87% had developed thoracic aortic dissection and 13% had developed abdominal aortic dissection.[12] However, it was unclear whether the mice with abdominal aortic dissection had also developed thoracic aortic dissection. Thus, it is important to describe the region of aortic dissection because concomitant thoracic and abdominal aortic dissection would suggest that the initiation of aortic dissection had started from the thoracic aortic region. In addition, the studies that had reported thoracic aortic dissection, most had not specified whether the aortic dissection had started in the ascending aortic region, aortic arch, or descending thoracic aortic region. The usefulness of this model would be enhanced by investigators including region-specific data, such as the aortic region of AAD initiation, the extension of the involved aortic regions, and the rupture location.

Molecular mechanisms of BAPN-induced AAD

Inflammation. BAPN administration provoked increased plasma concentrations of multiple inflammatory molecules, such as interleukin (IL)-1β, IL-2, IL-3, IL-6, CD40 ligand, and tumor necrosis factor-α.[50,56] A direct link of these increases to the development of aortopathies has been demonstrated by whole body deletion of either IL-3 or CD40 ligand that attenuated BAPN-induced AAD formation.[50,56] Also, deletion of complement C3a receptor inhibited the development of

Table II. Comparison of AAD between humans and BAPN-administered mice

Feature	Humans	BAPN-administered mice
Location		
Aneurysm	Abdominal > thoracic aorta	Thoracic > abdominal aorta
Dissection	Thoracic aorta	Thoracic aorta
False lumen formation	Media	Media
Elastin fragmentation	Yes	Yes
Collagen deposition	Yes	Yes
Inflammatory cell accumulation	Yes	Yes

AAD, Aortic aneurysm and dissection; *BAPN*, β-aminopropionitrile.

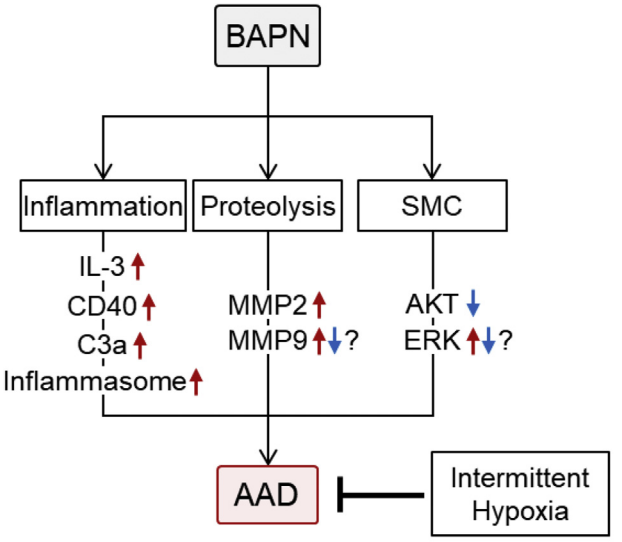

Fig 1. Molecular mechanisms studied in β-aminopropionitrile (BAPN)-induced aortic aneurysm and dissection (AAD) mouse model. *IL*, Interleukin; *MMP*, metalloproteinase; *SMC*, smooth muscle cell.

BAPN-induced AAD.[53] In addition, the anti-inflammatory compound, dexamethasone, attenuated BAPN-induced AAD, accompanied by diminished inflammation.[62] These findings support the idea that inflammation plays a critical role in the development of BAPN-induced AAD (Fig 1).

Metalloproteinase. Several studies have demonstrated changes in metalloproteinases (MMPs) in mouse aortas during BAPN administration, in particular, the gelatinases, MMP2 and MMP9. Some studies have uniformly demonstrated increased MMP2 protein and mRNA,[12,50,53,61,64] and aortic MMP9 protein was shown to increase in all[52,53,60,62,64] but two studies[12,50] (Fig 1). In addition to the gelatinases, several studies have reported an increase in aortic MMP3.[50,57,45] A causal role in the changes of MMP abundance can be inferred from the single study in which suppression of MMP2 using short hairpin RNA attenuated BAPN-induced AAD formation.[53] Although multiple studies have shown the contribution of MMPs to the pathophysiology of BAPN-induced AAD, it remains unknown how BAPN alters aortic MMPs. In addition, BAPN has been assumed to cause AAD through the inhibition of elastin and collagen crosslinking. Overall, the precise role of MMPs in BAPN-induced AAD formation remains to be clarified.

Smooth muscle cells. The loss of smooth muscle cells (SMCs) in BAPN-induced AAD has been attributed to apoptosis (Fig 1).[52,54,55,60-62] Consistent with the promotion of SMC apoptosis, AKT phosphorylation was downregulated in mice after BAPN administration.[52,60,79] However, phosphorylation of ERK is controversial in the BAPN-induced AAD mouse model.[62,79] A direct role of SMC apoptosis has been inferred by the effects of rapamycin that prevented BAPN-induced AAD formation. It is of note that intermittent hypoxia alleviated BAPN-induced AAD with inhibition of SMC apoptosis.[52] The effects of SMCs was also demonstrated by SMC-specific sirtuin-1 overexpression, which decreased the BAPN-induced AAD rupture rate.[64] Sirtuin-1 was reported to have antioxidative effects in the aorta.[81] Despite these studies, the mechanism by which BAPN induces SMC phenotypic changes has not yet been defined.

During the past decade, many molecular mechanisms by which BAPN causes AAD formation have been explored. However, many studies had used aortas harvested after 4 weeks of BAPN administration, which could have had overt pathology, such as aneurysms and dissections. Thus, it is difficult to discern whether the observed changes were a cause or a consequence of the aortic pathology. For greater insight, it is important to determine which changes are present at early intervals of BAPN administration before the appearance of overt pathology.

IMAGING TOOLS FOR DETECTING BAPN-INDUCED AAD

High-frequency ultrasound. With the advent of high-frequency ultrasound instruments, noninvasive ultrasound has been commonly used to monitor aortic dilation in mice.[82] Multiple studies have used ultrasound to assess BAPN-induced AAD.[52-54,56-58,60,61,47,48,79] Most studies had measured the luminal diameters in the proximal thoracic aorta as a parameter of AAD severity. Right and left parasternal approaches are the standard ultrasound modes for mice. However, these modes are not optimal for descending aortic imaging owing to interference from the lungs and ribs. A recent study reported a paraspinal dorsal approach for ultrasound imaging in the descending aortic region of mice (Fig 2, *A*).[48] This approach can visualize aortic dilatations

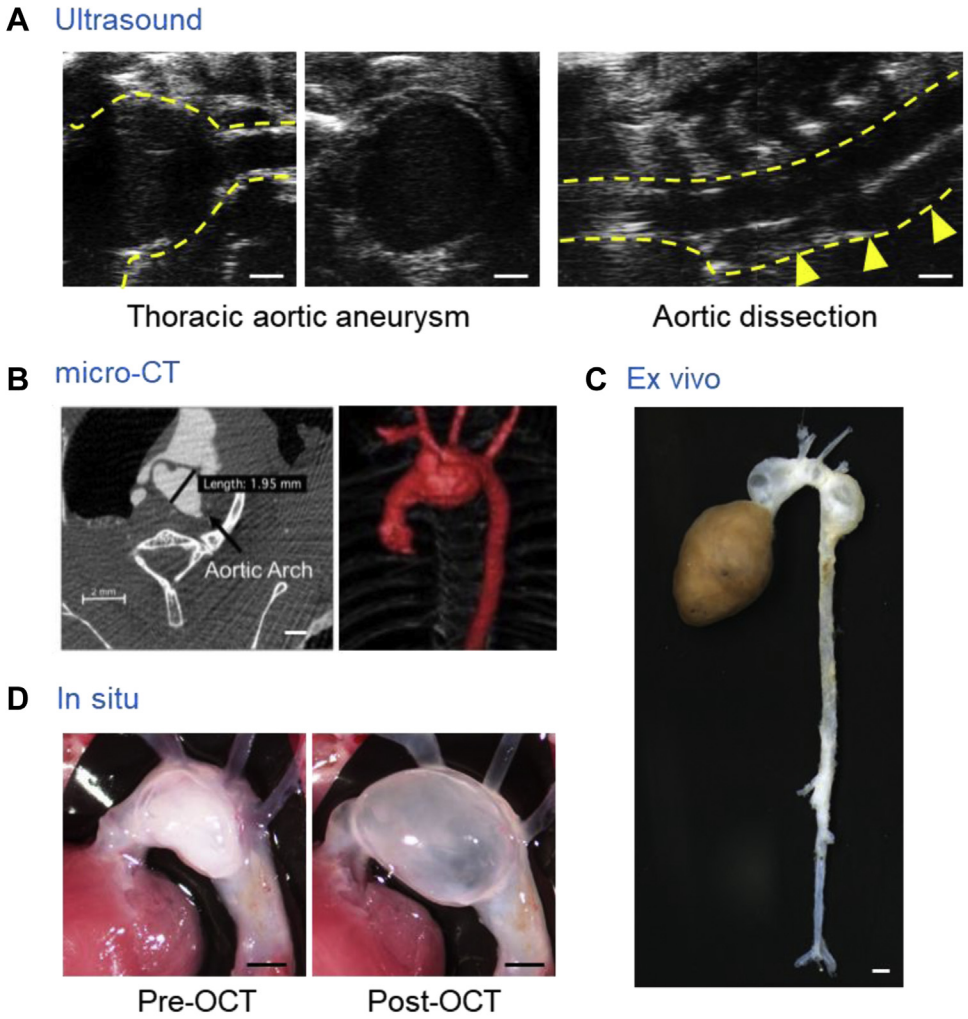

Fig 2. Imaging tools for detecting β-aminopropionitrile (BAPN-induced aortic aneurysm and dissection (AAD) in mice. Representative aortic images of ultrasound[48] **(A)**, micro-computed tomography (CT),[46] ex vivo (authors' unpublished data; **C**), and in situ[47] **(D)** approaches. *OCT,* Tissue-Tek optimal cutting temperature (compound; Sakura Finetek, Torrance, Calif). Scale bar = 1 mm.

and false lumen formation through the descending thoracic aorta of BAPN-administered mice (Fig 2, *A*).

Micro-computed tomography. Micro-computed tomography (CT) is a modality used for the acquisition of high-resolution aortic images of mice. Unlike ultrasound, micro-CT has less dependency on user skill for acquiring aortic images that can be used for quantitation of dimensions. In addition, micro-CT readily enables evaluation of the aortic size in three dimensions, which might provide more detailed structural information. Several studies have used micro-CT to detect BAPN-induced aneurysms at study termination (Fig 2, *B*).[61,46] Despite detailed information with high reliability, the necessity of an intravenous injection of contrast agent has impeded the use of serial micro-CT imaging studies. Sequential micro-CT monitoring has not been reported for BAPN-administered mice. Because BAPN leads to heterogeneous aortic pathologies, it would be interesting to monitor BAPN-induced AAD formation sequentially using micro-CT in live animals.

Magnetic resonance imaging. The mouse aorta can also be visualized using magnetic resonance imaging (MRI).[83] MRI does not result in radiation exposure and might not require contrast agents for basic imaging of mouse aortas. One study using MRI showed overt dilatation of the proximal thoracic aorta in BAPN-administered mice that was consistent with the ultrasound and ex vivo findings.[53] However, the spatial resolution of MRI is not sufficient to assess small structural alterations in mouse aortas. Its expense is also a barrier to the use of MRI. Thus, at present, MRI cannot be routinely applied for evaluating aortic morphology in mice.

Ex vivo and in situ imaging. Ex vivo approaches have been used most frequently to evaluate BAPN-induced AAD in mice (Fig 2, *C*).[12,47,48,52-61,63,64,79] BAPN induces

heterogeneous aortic pathologies in the entire thoracic aorta. Because ex vivo approaches can detect AAD directly in any region, it has advantages for the evaluation of aortic pathologies in BAPN-administered mice. However, owing to the absence of blood pressure, it is difficult to maintain the aortic dimensions after euthanasia, especially when severe pathologies are present. Therefore, formalin or latex perfusion has been used frequently to maintain aortic patency during ex vivo imaging.[84-86] In situ imaging has also been a common approach for aortic evaluations in mice.[47,48,87] This approach can assess aortic morphology while the tissue resides in the anatomic position. A recent study demonstrated the reliability of aortic measurements using in situ images with optimal cutting temperature compound infused into BAPN-induced AAD.[47] Optimal cutting temperature compound injection expanded the aortic lumen, and the aortic diameters were comparable to the ultrasound measurements (Fig 2, *D*). It is worth noting that the aortic diameters using ex vivo or in situ images are external, not luminal, diameters. Because external diameters will not correspond to luminal diameters in aortic dissections, other modalities, including ultrasound and micro-CT, could be considered to assess the luminal diameters in addition to external diameters.

Several modalities and methods are available to evaluate aortic morphology in mice. Because each approach has different advantages and shortcomings, the imaging approaches should be chosen to optimize the endpoints of each study. In addition, the heterogeneity of BAPN-induced aortic pathologies has resulted in challenges to aortic imaging for the acquisition of authentic measurements. Therefore, for robust evaluations, we would recommend the use of multiple modes to validate BAPN-induced aortic pathologies in mice.

SUMMARY AND PERSPECTIVES

BAPN-induced AAD replicates a spectrum of the features of human AAD (Table II). Thus, this mouse model provides opportunities to study the complex mechanisms of AAD from the early to advanced stages for exploring potential therapies. Although much research is required to translate animal findings into human uses, advances in research tools, including state-of-the-art imaging systems and well-controlled pharmacologic studies, will provide insights into defining therapies for AAD. Prospectively, collaborations between basic science investigators and physician scientists will enhance our knowledge of AAD mechanisms and pathophysiology in humans and provide ultimate insights into translating the findings from animal studies into human uses.

AUTHOR CONTRIBUTIONS

Conception and design: AD, HL
Analysis and interpretation: HS, AD, HL
Data collection: HS, ZB, SI, HL
Writing the article: HS, AD, HL
Critical revision of the article: HS, ZB, SI, AD, HL
Final approval of the article: HS, ZB, SI, AD, HL
Statistical analysis: Not applicable
Obtained funding: AD
Overall responsibility: HL

REFERENCES

1. Milewicz DM, Ramirez F. Therapies for thoracic aortic aneurysms and acute aortic dissections. Arterioscler Thromb Vasc Biol 2019;39:126-36.
2. Clough RE, Nienaber CA. Management of acute aortic syndrome. Nat Rev Cardiol 2015;12:103-14.
3. Nienaber CA, Clough RE. Management of acute aortic dissection. Lancet 2015;385:800-11.
4. Thompson MM. Infrarenal abdominal aortic aneurysms. Curr Treat Options Cardiovasc Med 2003;5:137-46.
5. Isselbacher EM. Thoracic and abdominal aortic aneurysms. Circulation 2005;111:816-28.
6. Albornoz G, Coady MA, Roberts M, Davies RR, Tranquilli M, Rizzo JA, et al. Familial thoracic aortic aneurysms and dissections—incidence, modes of inheritance, and phenotypic patterns. Ann Thorac Surg 2006;82:1400-5.
7. Waibel PE, Pomeroy BS. Effect of diet on the development of beta-aminopropionitrile-induced vascular hemorrhage in turkeys. J Nutr 1959;67:275-88.
8. McKay GF, Lalich JJ, Schilling ED, Strong FM. A crystalline "lathyrus factor" from Lathyrus odoratus. Arch Biochem Biophys 1954;52:313-22.
9. Levene CI. Studies on the mode of action of lathyrogenic compounds. J Exp Med 1962;116:119-30.
10. O'Dell BL, Elsden DF, Thomas J, Partridge SM, Smith RH, Palmer R. Inhibition of the biosynthesis of the cross-links in elastin by a lathyrogen. Nature 1966;209:401-2.
11. Pinnell SR, Martin GR, Miller EJ. Desmosine biosynthesis: nature of inhibition by D-penicillamine. Science 1968;161:475-6.
12. Ren W, Liu Y, Wang X, Jia L, Piao C, Lan F, et al. β-Aminopropionitrile monofumarate induces thoracic aortic dissection in C57BL/6 mice. Sci Rep 2016;6:28149.
13. Zheng HQ, Rong JB, Ye FM, Xu YC, Lu HS, Wang JA. Induction of thoracic aortic dissection: a mini-review of β-aminopropionitrile-related mouse models. J Zhejiang Univ Sci B 2020;21:603-10.
14. Jiang DS, Yi X, Zhu XH, Wei X. Experimental in vivo and ex vivo models for the study of human aortic dissection: promises and challenges. Am J Transl Res 2016;8:5125-40.
15. Shen YH, LeMaire SA. Molecular pathogenesis of genetic and sporadic aortic aneurysms and dissections. Curr Probl Surg 2017;54:95-155.
16. Staiculescu MC, Kim J, Mecham RP, Wagenseil JE. Mechanical behavior and matrisome gene expression in the aneurysm-prone thoracic aorta of newborn lysyl oxidase knockout mice. Am J Physiol Heart Circ Physiol 2017;313:H446-56.
17. Lee VS, Halabi CM, Hoffman EP, Carmichael N, Leshchiner I, Lian CG, et al. Loss of function mutation in LOX causes thoracic aortic aneurysm and dissection in humans. Proc Natl Acad Sci U S A 2016;113:8759-64.
18. Narayanan AS, Siegel RC, Martin GR. On the inhibition of lysyl oxidase by β-aminopropionitrile. Biochem Biophys Res Commun 1972;46:745-51.
19. Tang SS, Simpson DE, Kagan HM. Beta-substituted ethylamine derivatives as suicide inhibitors of lysyl oxidase. J Biol Chem 1984;259:975-9.
20. Jung ST, Kim MS, Seo JY, Kim HC, Kim Y. Purification of enzymatically active human lysyl oxidase and lysyl oxidase-like protein from *Escherichia coli* inclusion bodies. Protein Expr Purif 2003;31:240-6.
21. Hajdú I, Kardos J, Major B, Fabó G, Lőrincz Z, Cseh S, et al. Inhibition of the LOX enzyme family members with old and new ligands: selectivity analysis revisited. Bioorg Med Chem Lett 2018;28:3113-8.
22. Kanematsu Y, Kanematsu M, Kurihara C, Tsou TL, Nuki Y, Liang EI, et al. Pharmacologically induced thoracic and abdominal aortic aneurysms in mice. Hypertension 2010;55:1267-74.

23. Kurihara T, Shimizu-Hirota R, Shimoda M, Adachi T, Shimizu H, Weiss SJ, et al. Neutrophil-derived matrix metalloproteinase 9 triggers acute aortic dissection. Circulation 2012;126:3070-80.
24. Lu G, Su G, Davis JP, Schaheen B, Downs E, Roy RJ, et al. A novel chronic advanced stage abdominal aortic aneurysm murine model. J Vasc Surg 2017;66:232-42.e4.
25. Romary DJ, Berman AG, Goergen CJ. High-frequency murine ultrasound provides enhanced metrics of BAPN-induced AAA growth. Am J Physiol Heart Circ Physiol 2019;317:H981-90.
26. Anzai A, Shimoda M, Endo J, Kohno T, Katsumata Y, Matsuhashi T, et al. Adventitial CXCL1/G-CSF expression in response to acute aortic dissection triggers local neutrophil recruitment and activation leading to aortic rupture. Circ Res 2015;116:612-23.
27. Fyfe FW, Gillman T, Oneson IB. A combined quantitative chemical, light, and electron microscope study of aortic development in normal and nitrile-treated mice: possible implications for elucidating nitrile-induced aortic lesions and regarding the genesis of spontaneous arterial lesions. Ann N Y Acad Sci 1968;149:591-627.
28. Groth KA, Stochholm K, Hove H, Kyhl K, Gregersen PA, Vejlstrup N, et al. Aortic events in a nationwide Marfan syndrome cohort. Clin Res Cardiol 2017;106:105-12.
29. Trolle C, Mortensen KH, Hjerrild BE, Cleemann L, Gravholt CH. Clinical care of adult Turner syndrome—new aspects. Pediatr Endocrinol Rev 2012;9(Suppl 2):739-49.
30. Eagleton MJ. Arterial complications of vascular Ehlers-Danlos syndrome. J Vasc Surg 2016;64:1869-80.
31. Izawa-Ishizawa Y, Imanishi M, Zamami Y, Toya H, Nagao T, Morishita M, et al. Development of a novel aortic dissection mouse model and evaluation of drug efficacy using in-vivo assays and database analyses. J Hypertens 2019;37:73-83.
32. Kurobe H, Hirata Y, Matsuoka Y, Sugasawa N, Higashida M, Nakayama T, et al. Protective effects of selective mineralocorticoid receptor antagonist against aortic aneurysm progression in a novel murine model. J Surg Res 2013;185:455-62.
33. Kurobe H, Matsuoka Y, Hirata Y, Sugasawa N, Maxfield MW, Sata M, et al. Azelnidipine suppresses the progression of aortic aneurysm in wild mice model through anti-inflammatory effects. J Thorac Cardiovasc Surg 2013;146:1501-8.
34. Logghe G, Trachet B, Aslanidou L, Villaneuva-Perez P, De Backer J, Stergiopulos N, et al. Propagation-based phase-contrast synchrotron imaging of aortic dissection in mice: from individual elastic lamella to 3D analysis. Sci Rep 2018;8:2223.
35. Nishida N, Aoki H, Ohno-Urabe S, Nishihara M, Furusho A, Hirakata S, et al. High salt intake worsens aortic dissection in mice: involvement of IL (interleukin)-17A-dependent ECM (extracellular matrix) metabolism. Arterioscler Thromb Vasc Biol 2020;40:189-205.
36. Tomida S, Aizawa K, Nishida N, Aoki H, Imai Y, Nagai R, et al. Indomethacin reduces rates of aortic dissection and rupture of the abdominal aorta by inhibiting monocyte/macrophage accumulation in a murine model. Sci Rep 2019;9:10751.
37. Li X, Liu D, Zhao L, Wang L, Li Y, Cho K, et al. Targeted depletion of monocyte/macrophage suppresses aortic dissection with the spatial regulation of MMP-9 in the aorta. Life Sci 2020;254:116927.
38. Chen JY, Tsai PJ, Tai HC, Tsai RL, Chang YT, Wang MC, et al. Increased aortic stiffness and attenuated lysyl oxidase activity in obesity. Arterioscler Thromb Vasc Biol 2013;33:839-46.
39. Lu H, Howatt DA, Balakrishnan A, Moorleghen JJ, Rateri DL, Cassis LA, et al. Subcutaneous angiotensin II infusion using osmotic pumps induces aortic aneurysms in mice. J Vis Exp 2015;103:53191.
40. Daugherty A, Manning MW, Cassis LA. Angiotensin II promotes atherosclerotic lesions and aneurysms in apolipoprotein E-deficient mice. J Clin Invest 2000;105:1605-12.
41. Sevil MB, Anadon-Baselga MJ, Frejo MT, Llama E, Capo MA. Pharmacokinetic analysis of beta-aminopropionitrile in rabbits. Vet Res 1996;27:117-23.
42. Obama T, Tsuji T, Kobayashi T, Fukuda Y, Takayanagi T, Taro Y, et al. Epidermal growth factor receptor inhibitor protects against abdominal aortic aneurysm in a mouse model. Clin Sci (Lond) 2015;128:559-65.
43. Qi X, Wang F, Chun C, Saldarriaga L, Jiang Z, Pruitt EY, et al. A validated mouse model capable of recapitulating the protective effects of female sex hormones on ascending aortic aneurysms and dissections (AADs). Physiol Rep 2020;8:e14631.
44. Bachmanov AA, Reed DR, Beauchamp GK, Tordoff MG. Food intake, water intake, and drinking spout side preference of 28 mouse strains. Behav Genet 2002;32:435-43.
45. Aicher BO, Zhang J, Muratoglu S, Galisteo R, Arai AL, Gray VL, et al. Moderate aerobic exercise prevents matrix degradation and death in a mouse model of aortic dissection and aneurysm. Am J Physiol Heart Circ Physiol 2021;320:H1786-801.
46. Aicher BO, Mukhopadhyay S, Lu X, Muratoglu SC, Strickland DK, Ucuzian AA. Quantitative micro-CT analysis of aortopathy in a mouse model of β-aminopropionitrile-induced aortic aneurysm and dissection. J Vis Exp 2018;137:57589.
47. Ohno-Urabe S, Kukida M, Franklin MK, Katsumata Y, Su W, Gong MC, et al. Authentication of in situ measurements for thoracic aortic aneurysms in mice. Arterioscler Thromb Vasc Biol 2021;41:2117-9.
48. Sawada H, Franklin MK, Moorleghen JJ, Howatt DA, Kukida M, Lu HS, et al. Ultrasound monitoring of descending aortic aneurysms and dissections in mice. Arterioscler Thromb Vasc Biol 2020;40:2557-9.
49. Chen Y, Wei X, Zhang Z, He Y, Huo B, Guo X, et al. Downregulation of filamin A expression in the aorta is correlated with aortic dissection. Front Cardiovasc Med 2021;8:690846.
50. Liu C, Zhang C, Jia L, Chen B, Liu L, Sun J, et al. Interleukin-3 stimulates matrix metalloproteinase 12 production from macrophages promoting thoracic aortic aneurysm/dissection. Clin Sci (Lond) 2018;132:655-68.
51. Zhang WM, Liu Y, Li TT, Piao CM, Liu O, Liu JL, et al. Sustained activation of ADP/P2ry12 signaling induces SMC senescence contributing to thoracic aortic aneurysm/dissection. J Mol Cell Cardiol 2016;99:76-86.
52. Yang YY, Li LY, Jiao XL, Jia LX, Zhang XP, Wang YL, et al. Intermittent hypoxia alleviates β-aminopropionitrile monofumarate induced thoracic aortic dissection in C57BL/6 mice. Eur J Vasc Endovasc Surg 2020;59:1000-10.
53. Ren W, Liu Y, Wang X, Piao C, Ma Y, Qiu S, et al. The complement C3a-C3aR axis promotes development of thoracic aortic dissection via regulation of MMP2 expression. J Immunol 2018;200:1829-38.
54. Jia LX, Zhang WM, Zhang HJ, Li TT, Wang YL, Qin YW, et al. Mechanical stretch-induced endoplasmic reticulum stress, apoptosis and inflammation contribute to thoracic aortic aneurysm and dissection. J Pathol 2015;236:373-83.
55. Jia LX, Zhang WM, Li TT, Liu Y, Piao CM, Ma YC, et al. ER stress dependent microparticles derived from smooth muscle cells promote endothelial dysfunction during thoracic aortic aneurysm and dissection. Clin Sci (Lond) 2017;131:1287-99.
56. Han L, Dai L, Zhao YF, Li HY, Liu O, Lan F, et al. CD40L promotes development of acute aortic dissection via induction of inflammation and impairment of endothelial cell function. Aging (Albany NY) 2018;10:371-85.
57. Shao Y, Li G, Huang S, Li Z, Qiao B, Chen D, et al. Effects of extracellular matrix softening on vascular smooth muscle cell dysfunction. Cardiovasc Toxicol 2020;20:548-56.
58. Xu K, Xu C, Zhang Y, Qi F, Yu B, Li P, et al. Identification of type IV collagen exposure as a molecular imaging target for early detection of thoracic aortic dissection. Theranostics 2018;8:437-49.
59. Wang S, Liu Y, Zhao G, He L, Fu Y, Yu C, et al. Postnatal deficiency of ADAMTS1 ameliorates thoracic aortic aneurysm and dissection in mice. Exp Physiol 2018;103:1717-31.
60. Zhou B, Li W, Zhao G, Yu B, Ma B, Liu Z, et al. Rapamycin prevents thoracic aortic aneurysm and dissection in mice. J Vasc Surg 2019;69:921-32.e3.
61. Xia L, Sun C, Zhu H, Zhai M, Zhang L, Jiang L, et al. Melatonin protects against thoracic aortic aneurysm and dissection through SIRT1-dependent regulation of oxidative stress and vascular smooth muscle cell loss. J Pineal Res 2020;69:e12661.
62. Wang X, Zhang X, Qiu T, Yang Y, Li Q, Zhang X. Dexamethasone reduces the formation of thoracic aortic aneurysm and dissection in a murine model. Exp Cell Res 2021;405:112703.
63. Gao Y, Wang Z, Zhao J, Sun W, Guo J, Yang Z, et al. Involvement of B cells in the pathophysiology of β-aminopropionitrile-induced thoracic aortic dissection in mice. Exp Anim 2019;68:331-9.
64. Wang F, Tu Y, Gao Y, Chen H, Liu J, Zheng J. Smooth muscle sirtuin 1 blocks thoracic aortic aneurysm/dissection development in mice. Cardiovasc Drugs Ther 2020;34:641-50.
65. Miana M, Galan M, Martinez-Martinez E, Varona S, Jurado-Lopez R, Bausa-Miranda B, et al. The lysyl oxidase inhibitor beta-

aminopropionitrile reduces body weight gain and improves the metabolic profile in diet-induced obesity in rats. Dis Model Mech 2015;8:543-51.
66. Xing C, Jiang D, Liu Y, Tang Q, Huang H. Lysyl oxidase inhibition enhances browning of white adipose tissue and adaptive thermogenesis. Genes Dis 2020;9:140-50.
67. Simon MM, Greenaway S, White JK, Fuchs H, Gailus-Durner V, Wells S, et al. A comparative phenotypic and genomic analysis of C57BL/6J and C57BL/6N mouse strains. Genome Biol 2013;14:R82.
68. Wortmann M, Arshad M, Peters AS, Hakimi M, Bockler D, Dihlmann S. The C57Bl/6J mouse strain is more susceptible to angiotensin II-induced aortic aneurysm formation than C57Bl/6N. Atherosclerosis 2020;318:8-13.
69. Lemaire SA, McDonald ML, Guo DC, Russell L, Miller CC III, Johnson RJ, et al. Genome-wide association study identifies a susceptibility locus for thoracic aortic aneurysms and aortic dissections spanning FBN1 at 15q21.1. Nat Genet 2011;43:996-1000.
70. Hagan PG, Nienaber CA, Isselbacher EM, Bruckman D, Karavite DJ, Russman PL, et al. The International Registry of Acute Aortic Dissection (IRAD): new insights into an old disease. JAMA 2000;283:897-903.
71. Nienaber CA, Fattori R, Mehta RH, Richartz BM, Evangelista A, Petzsch M, et al. Gender-related differences in acute aortic dissection. Circulation 2004;109:3014-21.
72. Liang NL, Genovese EA, Al-Khoury GE, Hager ES, Makaroun MS, Singh MJ. Effects of gender differences on short-term outcomes in patients with type B aortic dissection. Ann Vasc Surg 2017;38:78-83.
73. Deery SE, Shean KE, Wang GJ, Black JH, Upchurch GR Jr, Giles KA, et al. Female sex independently predicts mortality after thoracic endovascular aortic repair for intact descending thoracic aortic aneurysms. J Vasc Surg 2017;66:2-8.
74. Zhang X, Thatcher SE, Rateri DL, Bruemmer D, Charnigo R, Daugherty A, et al. Transient exposure of neonatal female mice to testosterone abrogates the sexual dimorphism of abdominal aortic aneurysms. Circ Res 2012;110:e73-85.
75. Henriques T, Zhang X, Yiannikouris FB, Daugherty A, Cassis LA. Androgen increases AT1a receptor expression in abdominal aortas to promote angiotensin II-induced AAAs in apolipoprotein E-deficient mice. Arterioscler Thromb Vasc Biol 2008;28:1251-6.
76. Tashima Y, He H, Cui JZ, Pedroza AJ, Nakamura K, Yokoyama N, et al. Androgens accentuate TGF-beta dependent Erk/Smad activation during thoracic aortic aneurysm formation in Marfan syndrome male mice. J Am Heart Assoc 2020;9:e015773.
77. Zhang X, Thatcher S, Wu C, Daugherty A, Cassis LA. Castration of male mice prevents the progression of established angiotensin II-induced abdominal aortic aneurysms. J Vasc Surg 2015;61:767-76.
78. Fashandi AZ, Spinosa M, Salmon M, Su G, Montgomery W, Mast A, et al. Female mice exhibit abdominal aortic aneurysm protection in an established rupture model. J Surg Res 2020;247:387-96.
79. Le S, Zhang H, Huang X, Chen S, Wu J, Chen S, et al. PKM2 activator TEPP-46 attenuates thoracic aortic aneurysm and dissection by inhibiting NLRP3 inflammasome-mediated IL-1β secretion. J Cardiovasc Pharmacol Ther 2020;25:364-76.
80. Barrow MV, Simpson CF, Miller EJ. Lathyrism: a review. Q Rev Biol 1974;49:101-28.
81. Budbazar E, Rodriguez F, Sanchez JM, Seta F. The role of sirtuin-1 in the vasculature: focus on aortic aneurysm. Front Physiol 2020;11:1047.
82. Sawada H, Chen JZ, Wright BC, Moorleghen JJ, Lu HS, Daugherty A. Ultrasound imaging of the thoracic and abdominal aorta in mice to determine aneurysm dimensions. J Vis Exp 2019;145:e59013.
83. Weinreb DB, Aguinaldo JG, Feig JE, Fisher EA, Fayad ZA. Non-invasive MRI of mouse models of atherosclerosis. NMR Biomed 2007;20:256-64.
84. Gallo EM, Loch DC, Habashi JP, Calderon JF, Chen Y, Bedja D, et al. Angiotensin II-dependent TGF-beta signaling contributes to Loeys-Dietz syndrome vascular pathogenesis. J Clin Invest 2014;124:448-60.
85. Habashi JP, Judge DP, Holm TM, Cohn RD, Loeys BL, Cooper TK, et al. Losartan, an AT1 antagonist, prevents aortic aneurysm in a mouse model of Marfan syndrome. Science 2006;312:117-21.
86. Lin CJ, Staiculescu MC, Hawes JZ, Cocciolone AJ, Hunkins BM, Roth RA, et al. Heterogeneous cellular contributions to elastic laminae formation in arterial wall development. Circ Res 2019;125:1006-18.
87. Li W, Li Q, Jiao Y, Qin L, Ali R, Zhou J, et al. TGFBR2 disruption in postnatal smooth muscle impairs aortic wall homeostasis. J Clin Invest 2014;124:755-67.

Submitted Jun 19, 2021; accepted Dec 1, 2021.